ARTICLE

# Mutations in *IMPG2*, Encoding Interphotoreceptor Matrix Proteoglycan 2, Cause Autosomal-Recessive Retinitis Pigmentosa

Dikla Bandah-Rozenfeld,[1,15] Rob W.J. Collin,[2,3,4,15] Eyal Banin,[1] L. Ingeborgh van den Born,[5] Karlien L.M. Coene,[2,4] Anna M. Siemiatkowska,[2,4] Lina Zelinger,[1] Muhammad I. Khan,[2,6] Dirk J. Lefeber,[7,8] Inbar Erdinest,[1] Francesco Testa,[9] Francesca Simonelli,[9] Krysta Voesenek,[2] Ellen A.W. Blokland,[2] Tim M. Strom,[10] Caroline C.W. Klaver,[11,12] Raheel Qamar,[6,13] Sandro Banfi,[14] Frans P.M. Cremers,[2,4] Dror Sharon,[1,16,*] and Anneke I. den Hollander[2,3,4,16,*]

Retinitis pigmentosa (RP) is a heterogeneous group of inherited retinal diseases caused by progressive degeneration of the photoreceptor cells. Using autozygosity mapping, we identified two families, each with three affected siblings sharing large overlapping homozygous regions that harbored the *IMPG2* gene on chromosome 3. Sequence analysis of *IMPG2* in the two index cases revealed homozygous mutations cosegregating with the disease in the respective families: three affected siblings of Iraqi Jewish ancestry displayed a nonsense mutation, and a Dutch family displayed a 1.8 kb genomic deletion that removes exon 9 and results in the absence of seven amino acids in a conserved SEA domain of the IMPG2 protein. Transient transfection of COS-1 cells showed that a construct expressing the wild-type SEA domain is properly targeted to the plasma membrane, whereas the mutant lacking the seven amino acids appears to be retained in the endoplasmic reticulum. Mutation analysis in ten additional index cases that were of Dutch, Israeli, Italian, and Pakistani origin and had homozygous regions encompassing *IMPG2* revealed five additional mutations; four nonsense mutations and one missense mutation affecting a highly conserved phenylalanine residue. Most patients with *IMPG2* mutations showed an early-onset form of RP with progressive visual-field loss and deterioration of visual acuity. The patient with the missense mutation, however, was diagnosed with maculopathy. The *IMPG2* gene encodes the interphotoreceptor matrix proteoglycan IMPG2, which is a constituent of the interphotoreceptor matrix. Our data therefore show that mutations in a structural component of the interphotoreceptor matrix can cause arRP.

## Introduction

Retinitis pigmentosa (RP) (MIM #268000), with a worldwide prevalence of about 1:4,000,[1–3] is a group of hereditary retinal degenerative diseases and is considered one of the most heterogeneous genetic diseases in humans. The retinal phenotype in patients with RP is usually caused by progressive degeneration of the rod photoreceptor cells and the subsequent degeneration of cones. This results in night blindness followed by gradual loss of visual fields and visual acuity and often progresses to blindness by the end of the sixth decade of life.[4] The disease presents with different modes of inheritance, including autosomal-recessive (50%–60% of cases), autosomal-dominant (30%–40% of cases), and X-linked (5%–15% of cases).[5] A total of 27 genes have so far been found to cause nonsyndromic autosomal-recessive RP (arRP), and four additional loci have been identified by linkage studies (see the RetNet database). The heterogeneity of RP is characterized not only by the large number of causative genes but also by the variable mechanisms in which the encoded proteins participate; such mechanisms include the phototransduction pathway, vitamin A metabolism, and the splicing machinery.[5] During the last two decades, two main methods have been used for identifying arRP genes: the candidate gene approach,[6] in which genes are screened for mutations mostly on the basis of the known or putative function of the encoded protein, and homozygosity mapping in large consanguineous families and subsequent mutation analysis of genes in the linked interval. Using these methods, researchers identified genes encoding proteins that are localized mainly to the photoreceptors and the retinal pigment epithelium (RPE). However, less attention was drawn to the retinal extracellular matrix (ECM), also known as the interphotoreceptor matrix (IPM), which fills the space between individual photoreceptor cells and between photoreceptors and the RPE. The IPM is a viscous material composed mainly of proteins,

[1]Department of Ophthalmology, Hadassah-Hebrew University Medical Center, Jerusalem, Israel; [2]Department of Human Genetics, Radboud University Nijmegen Medical Centre, Nijmegen, The Netherlands; [3]Department of Ophthalmology, Radboud University Nijmegen Medical Centre, Nijmegen, The Netherlands; [4]Nijmegen Centre for Molecular Life Sciences, Radboud University Nijmegen Medical Centre, Nijmegen, The Netherlands; [5]The Rotterdam Eye Hospital, Rotterdam, The Netherlands; [6]Department of Biosciences, COMSATS Institute of Information Technology, Islamabad, Pakistan; [7]Department of Neurology, Radboud University Nijmegen Medical Centre, Nijmegen, The Netherlands; [8]Department of Laboratory Medicine, Radboud University Nijmegen Medical Centre, Nijmegen, The Netherlands; [9]Department of Ophthalmology, Seconda Università degli Studi di Napoli, Naples, Italy; [10]Institute of Human Genetics, Helmholtz Zentrum Munchen, Neuherberg, Germany; [11]Department of Ophthalmology, Erasmus Medical Centre Rotterdam, The Netherlands; [12]Department of Epidemiology, Erasmus Medical Centre Rotterdam, The Netherlands; [13]Shifa College of Medicine, Islamabad, Pakistan; [14]Telethon Institute of Genetics and Medicine, Naples, Italy
[15]The first authors contributed equally
[16]The last authors contributed equally
*Correspondence: dror.sharon1@gmail.com (D.S.), a.denhollander@antrg.umcn.nl (A.I.d.H.)
DOI 10.1016/j.ajhg.2010.07.004. 

glycoproteins, and proteoglycans[7,8] and was considered for many years to serve as a glue between the photoreceptors and the RPE cells.[9] Data that has accumulated since then has revealed a broader IPM function, including intercellular communication, membrane turnover, regulation of neovascularization, cell survival, photoreceptor differentiation and maintenance, retinoid transport, and matrix turnover.[10,11] In addition, the IPM is thought to be important for the precise alignment of the photoreceptor cells to the optical light path.[12] A link between an abnormal IPM function and photoreceptor degeneration was obtained by a study in which inhibition of proteoglycan synthesis (by intravitreal injection of xyloside) caused both degeneration of the outer segment of cone photoreceptors and retinal detachment.[13] Only a few genes encoding proteins that are known or speculated to be localized to the IPM had thus far been associated with a retinal disease. These included *TIMP3* (MIM *188826), causing Sorsby's fundus dystrophy[14] (MIM #136900); *EFEMP1* (MIM *601548), causing dominant Doyne's honeycomb retinal degeneration[15] (MIM #126600); *IRBP* (MIM *180290), causing arRP;[16] *EYS* (MIM *612424), causing arRP;[17,18] and *ADAM9* (MIM *602713), causing autosomal-recessive cone-rod degeneration (MIM #612775).[19]

In the current study we performed autozygosity mapping to identify novel genes for arRP and Leber congenital amaurosis (LCA), a more severe, congenital retinal disorder. We identified six patients from two families, one Israeli and one Dutch, who had homozygous regions with an overlapping interval of 7.3 Mb on chromosome 3. This region contains the retina-specific *IMPG2* gene encoding the interphotoreceptor matrix proteoglycan 2. Sequence analysis identified *IMPG2* mutations in both families. Further analysis of Israeli, Palestinian, and European RP families revealed five additional mutations in *IMPG2*, underlining the importance of the IPM in the pathogenesis of arRP.

## Subjects and Methods

### Families and Genetic Analysis

The tenets of the Declaration of Helsinki were followed, and informed consent was obtained from all participating patients prior to donation of a blood sample. Blood samples for DNA analysis were obtained from affected and unaffected family members. Genomic DNA was extracted from peripheral blood samples with the FlexiGene DNA kit (QIAGEN, Germany) or by a standard salting-out procedure.

### Clinical Evaluation

Complete ophthalmic examinations were performed in all patients with mutations in *IMPG2* and included both electroretinography (ERG) according to ISCEV standards[20] and fundus photography. For some patients, additional clinical tests consisting of visual-field measurements were conducted with Goldmann kinetic perimetry or Optical Coherence Tomography (OCT) performed with Heidelberg Spectralis equipment.

### Homozygosity Mapping and Mutation Detection

Whole-genome SNP analysis was performed with the Illumina 6K or Affymetrix 10K, 250K, 5.0, or 6.0 SNP arrays. Homozygous regions were calculated with Partek software, and parametric multipoint linkage analysis was performed with Allegro in the EasyLinkage software package. For fine mapping genomic regions of interest, microsatellite markers were genotyped in affected and unaffected family members. Primers for PCR amplification of the 19 exons and exon-intron boundaries of *IMPG2* were designed with Primer 3 software[21] (Table S1). PCR was performed on 50 ng of genomic DNA in 25 μl reactions with 35 cycles. PCR fragments were purified with Exo nuclease I and FastAP (Fermentas, Canada) or with 96-well PCR filter plates (Millipore), and mutation analysis was performed by direct sequencing of PCR products. To determine the boundaries of the genomic deletion that was detected in family W01-299, we performed PCR analysis by using combinations of several primers located in introns 8 and 9 of the *IMPG2* gene. Primer sequences used in this analysis are available on request.

### DNA Constructs

The coding sequence of human *IMPG2* (UniProt_ID Q9BXV3) was amplified by PCR from human retina Marathon-ready cDNA (Clontech, Mountain View, USA) with forward primer 5-GGGGACAAGTTTGTACAAAAAAGCAGGCTTCGCCGCCACCATGATTATGTTTCCTCTTTTTGG-3′ and reverse primer 5′-GGGGACCACTTTGTACAAGAAAGCTGGTCAACCTCTTCCACTTGTTGCTC-3′ containing adapters for Gateway cloning (underlined). Entry clones were generated by Gateway technology (Invitrogen, Leek, The Netherlands) according to the manufacturer's instructions. A construct that contains the first SEA domain of human IMPG2 (amino acids 239–349) was generated by PCR using the full-length IMPG2 entry clone as a template and using forward primer 5′-GGGGACAAGTTTGTACAAAAAAGCAGGCTTCGGTGAACAGATTGCAGAATTC-3′ and reverse primer 5′-GGGGACCACTTTGTACAAGAAAGCTGGTCTTAATAAACAACAGTGGGTTTATC-3′. From this construct, an entry clone containing a mutant SEA domain (without the seven amino acids encoded by exon 9, coined the ΔRSPKEND mutant) was generated via site-directed mutagenesis with primers 5′-CATAGTAAACATCTACGCCACTAAATTCAAGTACACG-3′ and 5′-CGTGTACTTGAATTTAGTGGCGTAGATGTTTACTATG-3′. The sequence of all entry clones was verified in sense and antisense directions with dye termination chemistry on a 3730 DNA analyzer (Applied Biosystems Inc., Nieuwerkerk aan de Ijssel, The Netherlands). Gateway technology was used for cloning the wild-type SEA domain and the ΔRSPKEND mutant construct into the pSeqTag expression vector that contains a cytomegalo virus promoter, a signal peptide sequence for entering the secretory pathway, the cDNA-encoding-enhanced cyan fluorescent protein (eCFP), and then the sequence of

**Table 1. Families with Homozygous Regions Encompassing *IMPG2***

| Family | Affected Individuals | Level of Consanguinity | Origin | SNP array type | Flanking SNPs | Size of Homozygous Region (Mb) | Mutation in *IMPG2* (Effect on Protein) |
|---|---|---|---|---|---|---|---|
| *MOL0764* | *3* | *First cousins* | *Iraqi Jew* | *Affy 10K* | *rs1036051; rs326333* | *38.0* | *c.635C > G (p.Ser212X)* |
| *W01-299* | *3* | *None* | *Dutch* | *Affy 250K* | *rs12330531; rs2290477* | *12.8* | *c.888-1554_908+274 del (p.Arg296_Asp302 del)* |
| MOL0097 | 1 | First cousins | Palestinian Muslim | Affy 10K | rs1351109; rs722813 | 24.8 | None |
| MOL0260 | 1 | First cousins | Israeli Muslim | Affy 10K | rs1523448; rs1259489 | 55.4 | None |
| MOL0317 | 1 | First cousins | Israeli Muslim | Affy 10K | rs2325036; rs2134655 | 28.0 | None |
| MOL0408 | 1 | Second cousins | Russian Jew | Affy 10K | rs831451; rs907931 | 58.5 | None |
| W08-0023 | 1 | First cousins | Dutch | Affy 5.0 | rs4677400; rs358912 | 80.8 | None |
| *W08-1378* | *2* | *Second cousins* | *Dutch* | *Affy 6.0* | *rs17018482; rs103218337* | *22.0* | *c.2716C>T (p.Arg906X)* |
| *NAP1* | *1* | *Second cousins* | *Italian* | *Affy 5.0* | *rs9289536; rs7630522* | *13.6* | *c.2890C>T (p.Arg964X)* |
| *NAP75* | *1* | *First cousins* | *Italian* | *Affy 5.0* | *rs301930; rs7625411* | *15.4* | *c.3262C>T (p.Arg1088X)* |
| *RP49* | *3* | *First cousins* | *Pakistan* | *Illumina 6K* | *rs1320173; rs1920325* | *42.3* | *c.1680T>A (p.Tyr560X)* |
| *MOL0732* | *1* | *First cousins* | *Israeli Christian Arab* | *Illumina 6K* | *rs877523; rs1997422* | *59.2* | *c.370T>C (p.Phe124Leu)* |

Families with mutations in *IMPG2* are indicated in italics. The pedigrees of families MOL0764 and W01-299 are shown in Figure 1.

interest, thereby yielding pSeqTag- IMPG2 SEA wild-type and pSeqTag-IMPG2 SEA ΔRSPKEND.

### Cell Culture, Transfections, and Fluorescence Microscopy

COS-1 cells were cultured at 37°C in DMEM (Sigma-Aldrich, Zwijndrecht, The Netherlands) supplemented with 10% fetal calf serum (Sigma-Aldrich), 100 IU/ml penicillin, 100 μg/ml streptomycin, 10 mM sodium pyruvate (Sigma-Aldrich), and 1% Glutamax (Sigma-Aldrich). Cells were seeded on coverslips, and Effectene (QIAGEN, Venlo, The Netherlands) was used for transfecting cells with pSeqTag IMPG2 SEA wild-type or pSeqTag IMPG2 SEA ΔRSPKEND. After 24 hr, cells were fixed in ice-cold methanol for 10 min, treated with 1% Triton X-100 in phosphate-buffered saline (PBS) for 5 min, and blocked in 2% bovine serum albumine in PBS for 20 min. Incubation with the primary antibody rabbit-α-protein disulfide-isomerase (PDI, Stressgen, Ann Arbor, Michigan, USA) was performed for 2 hr. After being washed in PBS, coverslips were stained with donkey-α-rabbit Alexa 568 (Invitrogen) for 45 min. Coverslips were washed again with PBS and briefly with milliQ before being mounted in Vectashield containing DAPI (Vector Laboratories, Burlingame, CA, USA). The localization of constructs was analyzed with a Zeiss Axio Imager Z1 fluorescence microscope equipped with a 63× objective lens.

### PNGaseF Assay

COS-1 cells were transfected with DNA constructs encoding either the wild-type IMPG2-SEA domain or the ΔRSPKEND mutant in the pSeqTag vector. After 24 hr, cells were lysed in lysis buffer (50 mM Tris-HCl [pH 7.5], 150 mM NaCl, and 0,5% Triton X-100) and supplemented with complete protease inhibitor cocktail (Roche Diagnostics, Mannheim, Germany), and lysates were cleared by centrifugation for 10 min at 4°C and 12,500 rpm. Part of the protein lysates were incubated overnight at 37°C with PNGaseF according to the manufacturer's protocol (New England Biolabs, Hitchin, UK). PNGaseF-treated and -untreated samples were run on a NuPAGE Novex 4%–12% Bis-Tris SDS-PAGE gel (Invitrogen). Proteins were transferred onto a nitrocellulose membrane, and the IMPG2 SEA wild-type or ΔRSPKEND mutant proteins were analyzed with the monoclonal mouse α-GFP primary antibody (Roche Diagnostics) that also exhibits reactivity against eCFP. As a secondary antibody, goat-α-mouse coupled to IRDye800 (Rockland Immunochemicals, Gilbertsville, PA, USA) was used. Signals were recorded on a Li-Cor Odyssey 2.1 infrared scanner.

## Results

### Homozygosity Mapping and Mutation Detection

Whole-genome SNP analysis of 381 RP and 193 LCA patients of Israeli, Palestinian, and European origins revealed two RP families in which the affected siblings shared a large homozygous region at 3q12 (Table 1). In these two families (MOL0764 and W01-299), the region on chromosome 3 was the only large region that was homozygous in all affected relatives. In family MOL0764, an Israeli family of Iraqi Jewish origin, the 38 Mb critical interval was flanked by rs1036051 and rs326333 (Figure 1A). Microsatellite analysis in the Dutch family W01-299, including parents and nonaffected siblings, revealed that this region segregated with the disease, and

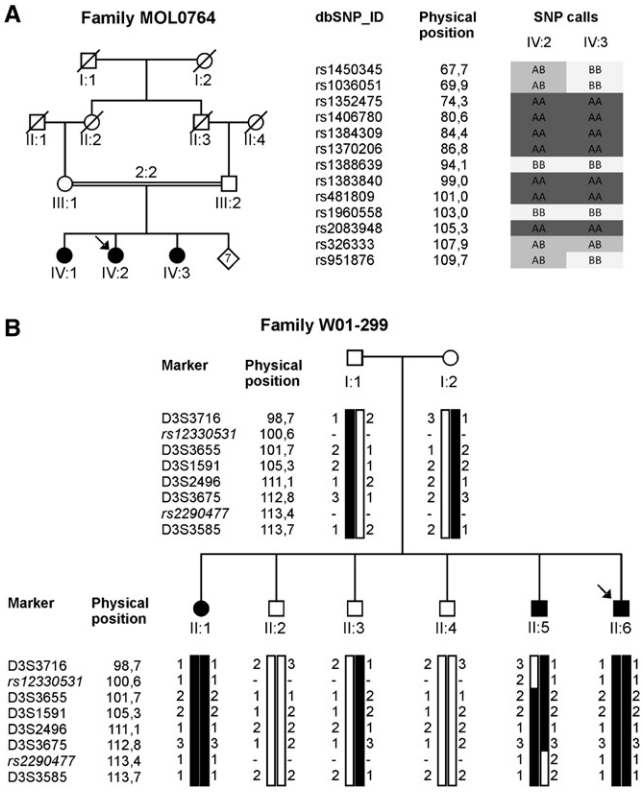


**Figure 1. Pedigrees and Segregation Analysis in Two Families with *IMPG2* Mutations**

(A) Family MOL0764: selected SNP markers encompassing the shared homozygous region in IV:2 and IV:3 as detected by the 10K Affymetrix array are shown in the right panel. The rs481809 marker is located within the *IMPG2* gene.

(B) Family W01-299: microsatellite and SNP analysis shows cosegregation of a chromosome-3q-linked haplotype with RP in family W01-299; the flanking SNPs are indicated in italics. Mutation-bearing haplotypes are marked by black bars.

Filled symbols represent affected individuals, whereas clear symbols represent unaffected individuals. The position of the markers (in Mb), based on the human genome browser GRCh37/hg19, is indicated.

a critical interval of 12.8 Mb, flanked by rs12330531 and rs2290477, was detected (Figure 1B). The overlapping interval of the two families spans 7.3 Mb, flanked by rs12330531 and rs326333 (Figure 2A). One of the 30 annotated genes in the overlapping region is the interphotoreceptor matrix proteoglycan 2 (*IMPG2*: MIM *607056) gene, which has previously been reported to be expressed specifically in the retina[22–24] and encodes a protein localized to the IPM.[22,23] *IMPG2* is speculated to be highly important for retinal adhesion[25] and therefore is an excellent candidate gene for retinal diseases.[26] Mutation analysis of *IMPG2* in the two probands of these families revealed two different disease-causing mutations. In family MOL0764, a homozygous nonsense mutation (c.635C > G; p.Ser212X) was identified in exon 6 (Figure 2D; Figure S1) in all three affected individuals. The mutation was not identified in 47 additional RP patients of Oriental Jewish origin (mainly from Iraq, Iran and Afghanistan), nor in 98 Israeli and Palestinian RP patients from other origins. The nonsense mutation was found heterozygously in one out of 104 controls of Oriental Jewish ancestry. In family W01-299, exon 9 of *IMPG2* failed to amplify in the affected individuals (Figure 2B, upper panel), suggesting the presence of a homozygous deletion. RT-PCR analysis of *IMPG2* cDNA derived from EBV-transformed lymphoblastoid cells revealed that exon 9 was absent from the mRNA in the affected individuals of family W01-299 (Figure 2C). Using several primer pairs located in introns 8 and 9 of *IMPG2*, we identified a 1850 bp genomic deletion that removes exon 9 (c.888-1554_908+274del) (Figure 2B, lower panel) and found that it segregated with RP (Figure 2B). The absence of exon 9 results in the deletion of seven amino acids (RSPKEND) from the encoded IMPG2 protein without affecting the reading frame (p.Arg296_Asp302 del; Figures 2C and 2D). The deletion was not present in 270 Dutch control individuals or in more than 700 probands who were of European origin and had isolated or autosomal-recessive RP.

In ten additional families with retinal disease, significant *IMPG2*-harboring homozygous regions, ranging from 13.6 to 80.8 Mb of genomic DNA, were identified (Table 1). Mutation analysis revealed five additional mutations in families from Israel, The Netherlands, Italy, and Pakistan; most of these mutations were associated with a diagnosis of RP (Table 1; Figure S1). In two Dutch siblings (family W08-1378), of which only the proband was genotyped on a SNP array, a homozygous nonsense mutation was identified (c.2716C>T; p.Arg906X). In two unrelated Italian RP patients from families NAP1 and NAP75, two additional homozygous nonsense mutations were identified (c.2890C>T; p.Arg964X and c.3262C>T; p.Arg1088X, respectively). In a Pakistani family (RP-49) with three affected individuals, another nonsense mutation was identified (c.1680T>A; p.Tyr560X). None of these mutations were identified in more than 100 ethnically matched control individuals, and each of them segregated with the disease in each of the families. The p.Arg906X mutation that was identified in the Dutch family W08-1378 was also present in a heterozygous state in an isolated RP patient from The Netherlands. However, no mutation on the second allele was detected by sequence analysis of all exons and intron-exon boundaries in this particular patient.

In addition, in an isolated patient who had maculopathy and was of Israeli Arab Christian origin, a homozygous nucleotide transition (c.370T>C) that is predicted to result in a missense mutation (p.Phe124Leu) (Figure S1) affecting a highly conserved phenylalanine residue (Figure 2E) was identified.

### Clinical Evaluation of Patients with *IMPG2* Mutations

Complete ophthalmic examinations were performed in all patients with mutations in *IMPG2*. In general, affected individuals with *IMPG2* mutations displayed typical symptoms and signs of RP; these included night

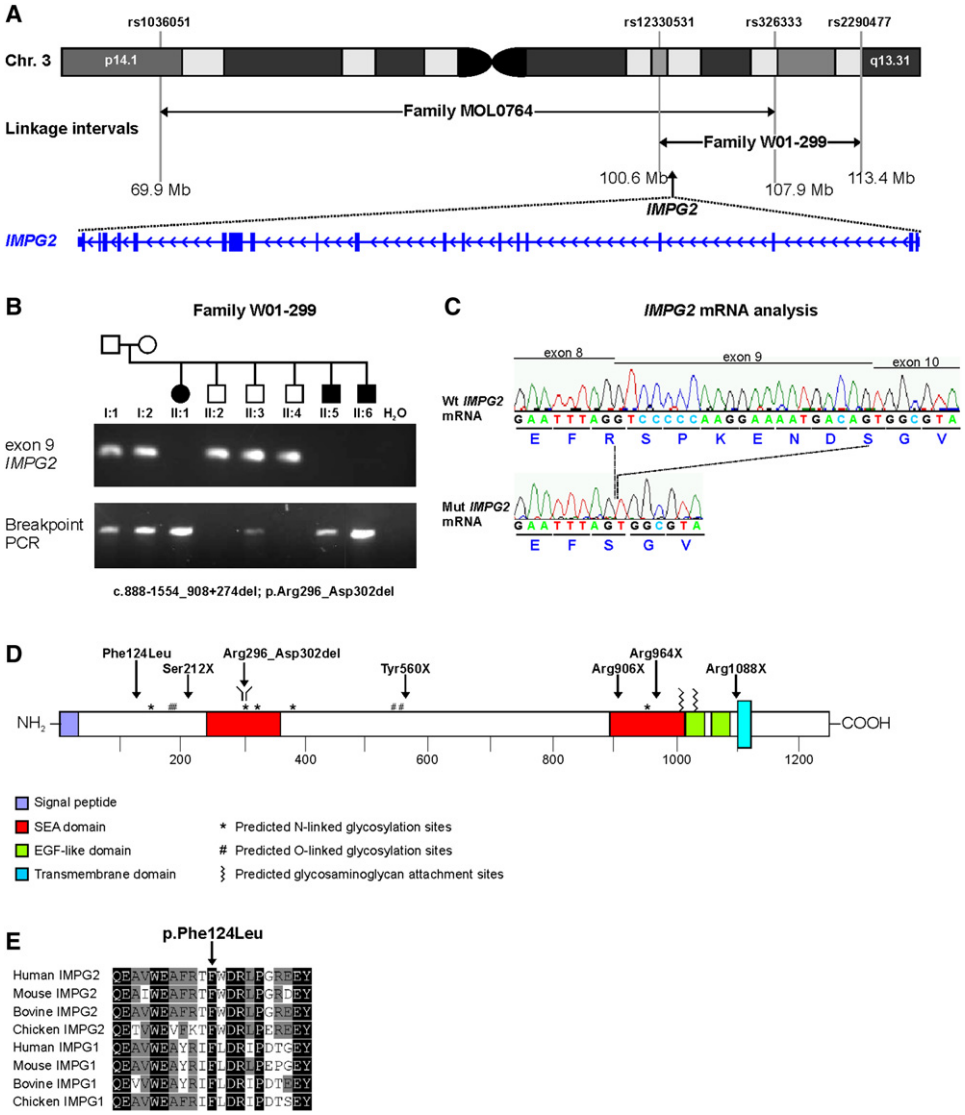


**Figure 2. Linkage Intervals, Mutation Analysis, and Protein Characterization of *IMPG2***

(A) Upper panel: part of chromosome 3 showing the linkage intervals and the corresponding flanking SNPs for arRP-families MOL0764 and W01-299. The genomic positions of these markers are indicated in Mb. *IMPG2* resides within the region that is shared by the two families. Lower panel: genomic structure of *IMPG2*; 19 exons are indicated as blue bars. The noncoding parts of exons 1 and 19 are indicated with a smaller bar.

(B) Upper panel: PCR analysis of exon 9 of *IMPG2*. Exon 9 was not amplified in the three affected individuals of family W01-299. All relatives and their position in the pedigree are indicated above the electropherogram. Lower panel: after identification of the breakpoints of the genomic deletion, PCR primers were designed to amplify a product if the deletion is present. This breakpoint PCR shows a product in all three affected individuals and in the heterozygous carriers, i.e., both parents (I:1 and I:2) and one unaffected brother (II:3).

(C) Sequence analysis of *IMPG2* mRNA derived from EBV-transformed cultured lymphoblasts of individual II:1 and of an unrelated control. RT-PCR and subsequent analysis shows that, because of the genomic deletion, exon 9 of *IMPG2* is absent in the mutant *IMPG2* mRNA. At the protein level, this is predicted to result in the absence of seven amino acids, i.e., RSPKEND.

(D) Graphical representation of the IMPG2 protein. Shown are the signal peptide, two SEA domains and two EGF-like domains in the large extracellular N-terminal part of the protein, and a transmembrane-spanning region. The positions of asparagine and threonine residues that are predicted to undergo N- or O-linked glycosylation, respectively, as well as the serine residues that might serve as core residues for the attachment of glycosaminoglycan side chains, are indicated with symbols described in the figure. The positions of the mutations identified in this study are indicated with arrows.

(E) Evolutionary conservation of the mutated phenylalanine residue and surrounding amino acids. Shown are partial protein sequences of human, mouse, bovine, and chicken IMPG2 and IMPG1 proteins. Amino acids that are identical in all proteins are presented in white on a black background, whereas partially conserved residues are shown in black on a gray background.

blindness, loss of the visual field, optic-disc pallor, attenuated vessels, and bone-spicule-like pigmentations. However, some inter- and intrafamilial variability was noted. The three sisters of family MOL0764 were diagnosed with RP and myopia at childhood and in their sixth decade had advanced RP with very low visual acuity (ranging from only the ability to count fingers to only the ability to perceive light), atrophic macular changes,

and severely constricted visual fields (Table 2, Figures 3A and 3B). In all three patients, full-field ERG responses were extinguished. The three affected siblings of family W01-299 were diagnosed with RP before the age of 15. Visual acuity varied from 20/125 to 20/32 at the time of presentation. The ERG responses in two of the siblings showed a rod-cone pattern and deteriorated over time. Posterior subcapsular cataracts led to cataract extraction in all three patients around the age of 30. All three featured a bull's-eye maculopathy (Figure 3C). The two affected siblings of family W08-1378 presented with early-onset night blindness and diminished color vision and were diagnosed with rod-cone dystrophy in their teens. At age 30, they both displayed moderate myopia, a waxy pallor of the optic disc, narrow vessels, some bone spicules in the periphery (Figures 3D–3G), and an undetectable ERG response (Table 2). The proband had a relatively intact macula with a visual acuity of 20/80 in both eyes and only loss of sensitivity in the central visual field. His younger brother, however, had patches of RPE atrophy in the macula (Figures 3F and 3G) and a visual acuity of 20/80 (right eye) and only enough visual acuity to count fingers (left eye), and visual-field testing showed a central scotoma in both eyes. The patient of family NAP1 was diagnosed with RP at the age of 30. Her clinical presentation in the late sixth decade of life showed advanced RP with atrophic macular changes, very low visual acuity, exotropia in the right eye, nystagmus, and posterior subcapsular cataracts, and her ERG was extinguished (Table 2). The patient of family NAP75 was diagnosed with RP during childhood, and in the sixth decade of life she had advanced RP with low visual acuity and atrophic macular changes. Her full-field ERG was extinguished, and the retinal degeneration was accompanied by posterior subcapsular cataracts that led to cataract extraction (Figure 3H, Table 2). In contrast to the patients with RP due to null mutations, patient MOL0732, with a homozygous missense mutation, was diagnosed with mild maculopathy at the age of 63. Her full-field ERG was within normal limits, her color vision was normal, and her best corrected visual acuity was 20/40 and 20/50 (Table 2). Fundus examination revealed a mild maculopathy (Figures S2A and S2B), and OCT analysis revealed elevation of the photoreceptor layer in the foveal region (Figures S2C and S2D). Visual-field testing revealed a relative central scotoma in the right eye, whereas in the left eye, the visual field was within normal limits.

### Functional Analysis of the ΔRSPKEND Mutation

To assess the consequences of the ΔRSPKEND mutation on the function of IMPG2, we analyzed the effect of the mutation on its glycosylation and protein trafficking. Using bioinformatic prediction programs for N- and mucin-type-O-linked glycosylation, we predicted that five asparagine residues (Asn154, Asn301, Asn320, Asn370, and Asn942) as well as four threonine residues (Thr190, Thr192, Thr544, and Thr556) would undergo N- and O-linked glycosylation, respectively (Figure 2D). In addition, two conserved serine residues have been found to serve as the core residues to which glycosaminoglycan side chains are attached (Figure 2D).[23] The seven amino acids deleted in the ΔRSPKEND mutant protein are located in the first SEA domain, which contains two predicted sites for the N-linked glycosylation of IMPG2. To determine whether the ΔRSPKEND mutant protein shows an impaired glycosylation, we subcloned the cDNA encoding the first SEA domain of IMPG2 into the pSeqTag vector both for the wild-type sequence and the ΔRSPKEND mutant. COS-1 cells were transiently transfected with the wild-type or the mutant construct, and 24 hr after transfection, cells were lysed and proteins were extracted. Part of the protein lysates were treated with PNGaseF, which removes N-linked carbohydrates, and subsequently subjected to SDS-PAGE. Immunoblot analysis showed no difference in migration of the proteins between PNGaseF-treated and -untreated lysates for either the wild-type or the ΔRSPKEND mutant IMPG2 protein (data not shown). These results indicate that the two asparagine residues that are predicted to undergo N-linked glycosylation are not glycosylated in COS-1 cells.

To determine whether the fusion proteins are properly targeted into the secretory pathway, we seeded COS-1 cells onto glass coverslips and transfected them with the same constructs. Fluorescence microscopy analysis showed that the fusion protein containing the wild-type IMPG2 SEA domain is present in vesicle-like structures in the endoplasmic reticulum (ER) and throughout the cytoplasm and is able to reach the cellular membrane (Figures 4A–4C). Intriguingly, the ΔRSPKEND mutant SEA domain appears to be trapped in the ER, which is observed as an accumulation of fluorescent protein adjacent to the nucleus, partially co-localizing with the ER-marker protein disulfide-isomerase (PDI) (Figure 4D–4F).

## Discussion

In this study, seven different mutations in *IMPG2* were identified in seven families of various ethnic origins. *IMPG2* encodes the retinal interphotoreceptor matrix proteoglycan IMPG2 (also known as IPM200 or SPACRCAN), that consists of 1,241 amino acids with a calculated molecular weight of 138.5 kDa.[22,24] The IMPG2 protein is highly similar to IMPG1 (also known as SPACR) and is predicted to contain a signal peptide, two SEA domains, and two EGF-like domains in the large extracellular N-terminal part of the protein, a putative transmembrane domain, and a cytoplasmic tail.[22,23] IMPG2 is synthesized by the photoreceptor cells and is secreted into the IPM. Both IMPG1 and IMPG2 have been shown to bind to hyaluronan, a glycosaminoglycan molecule that is essential for the organization of the IPM, and the sites for hyaluronan binding have been mapped in the mouse Impg2 protein.[25,27]

**Table 2. Clinical Characteristics of Patients with Mutations in *IMPG2***

| Patient | Age (yr) | Gender | Visual Acuity[a] | Refract. error[a,b] | Lens | Ophthalmoscopy | Goldmann Perimetry | ERG |
|---|---|---|---|---|---|---|---|---|
| MOL0764 IV:1 | 66 | F | LP<br>LP | −12.00<br>−11.75 | PSC and nuclear cataract | Posterior staphyloma, optic disc pallor, attenuated vessels, atrophic maculopathy, RPE atrophy with bone spicules in periphery | <5° | NR |
| MOL0764 IV:2 | 60 | F | HM<br>HM | −8.25<br>−5.50 | PSC cataract | Myopic changes, optic disc pallor, attenuated vessels, RPE atrophy in posterior pole and periphery with bone spicules | 5° | NR |
| MOL0764 IV:3 | 52 | F | CF<br>CF | −3.00<br>−3.25 | Mild PSC | Optic disc pallor, attenuated vessels, RPE atrophy in posterior pole and periphery with bone-spicules | Peripheral island | NR |
| W01-299 II:1 | 59 | F | LP<br>LP | −4.00[c]<br>−4.00[c] | IOL | Optic disc pallor, attenuated vessels, bull's-eye maculopathy, RPE atrophy with bone-spicules in periphery | n.p. | NR[d] |
| W01-299 II:5 | 45 | M | 20/200<br>LP | −0.25<br>−0.25 | IOL | Optic disc pallor, attenuated vessels with sheathing, subtle bull's eye maculopathywith ERM, RPE atrophy with bone-spicules in periphery | 10° RE,<br>LE n.p. | Significantly reduced, rod-cone pattern[e] |
| W01-299 II:6 | 44 | M | 20/200<br>20/200 | 0.00<br>+1.25 | IOL | Optic disc pallor, attenuated vessels, bull's-eye maculopathy, RPE atrophy with bone spicules in periphery | 10° | Significantly reduced, rod-cone pattern[f] |
| W08-1378 proband | 39 | M | 20/80<br>20/80 | −5.00<br>−6.75 | Mild cortical cataract | Optic disc pallor, attenuated vessels, relatively intact macula with bone spicules in periphery | Diminished sensitivity BE, LE small absolute scotoma in midperiphery | NR |
| W08-1378 affected brother | 36 | M | 20/80<br>CF | −3.50<br>−4.00 | Mild cortical cataract | Optic disc pallor, attenuated vessels, patchy RPE atrophy in macula with bone spicules in periphery | BE central and paracentral scotoma | NR |
| NAP1 proband | 68 | F | HM<br>HM | n.p[g] | PSC cataract | Optic disc pallor, attenuated vessels, atrophic maculopathy, RPE atrophy with bone spicules in periphery | n.p. | NR |
| NAP75 proband | 64 | F | 20/600<br>20/2400 | n.p[h] | pseudo-phakia | Optic disc pallor, attenuated vessels, atrophic maculopathy with ERM, RPE atrophy with bone spicules in periphery | n.p. | NR |
| RP-49 proband | 20 | M | n.p. | n.p | n.p. | Optic disc pallor, attenuated vessels, RPE atrophy with bone-spicules in periphery | n.p. | Significantly reduced, rod-cone pattern |
| MOL0732 proband | 63 | F | 20/40<br>20/50 | +2.25<br>+2.25 | Mild nuclear sclerosis | Mild maculopathy<br>RE > LE | RE central scotoma<br>LE within normal limits | Within normal limits |

Abbreviations are as follows: BE, both eyes; LE, left eye; RE, right eye; LP, light perception; HM, hand motion; CF, counting fingers; PSC, posterior subcapsular cataract; IOL, intra ocular lens; n.p., not performed; NR, nonrecordable; RPE, retinal pigment epithelium; and ERM, epiretinal membrane.
[a] The upper line represents the right eye, and the lower line represents the left eye.
[b] Spherical equivalent in Dioptres.
[c] Refractive error pre-cataract extraction
[d] ERGs performed at 8 and 27 years of age
[e] ERGS performed at 14 and 30 years of age
[f] ERGs performed at 12 and 23 years of age
[g] Refractive error pre-cataract extraction not available
[h] Refractive error not available because of advanced cataract

Five of the seven mutations found in this study introduce premature stop codons that will either result in nonsense-mediated degradation of the *IMPG2* mRNA or produce truncated IMPG2 proteins that would all lack the transmembrane domain and the cytoplasmic tail (Figure 2D). As such, these mutations can be considered

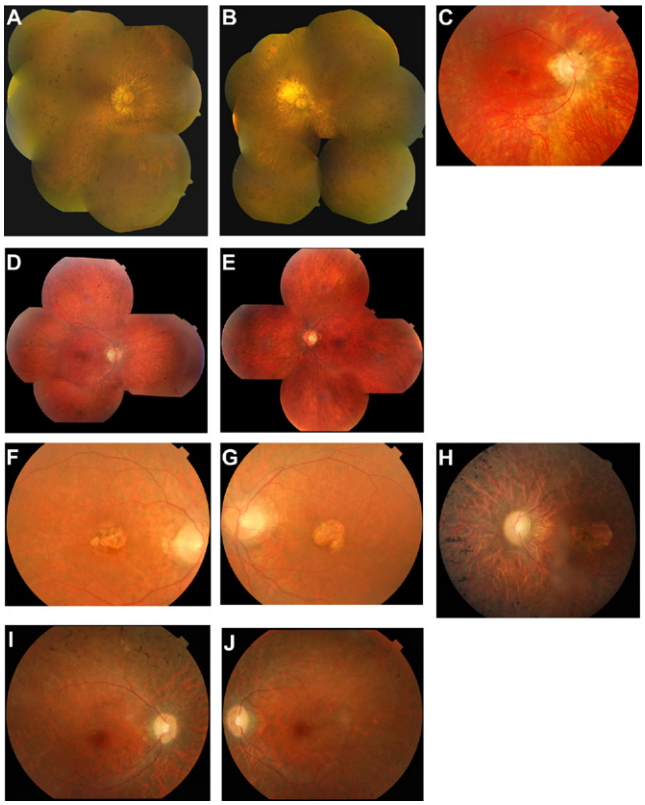


**Figure 3. Fundus Photographs of RP Patients with *IMPG2* Mutations**

(A and B) A montage of color fundus photos of MOL0764 IV:2 at age 60 shows advanced RP along with myopic changes.

(C) Fundus photographs of the right eye of patient W01-299 II:6, aged 44 years, show optic-disc pallor, attenuated vessels, bull's eye maculopathy, and mid-peripheral RPE atrophy with some intra-retinal pigmentations.

(D–G) Family W08-1378: (D and E) Montage of color fundus photos of the proband and (F and G) fundus photographs of the affected brother. Both show optic disc pallor, attenuated vessels, and patchy depigmentation of the RPE in the midperiphery with some bone spicules. Only the brother presented with sharply delineated atrophy of the RPE in the macula of both eyes.

(H) A fundus photograph of the left eye of proband NAP75, aged 64 years, shows optic-disc pallor, attenuated vessels, atrophic maculopathy, and mid-peripheral RPE atrophy with some intra-retinal pigmentations.

(I and J) A fundus photograph of both eyes of the proband of family RP-49 shows optic-disc pallor, attenuated vessels, and bone-spiculed pigmentations.

true loss-of-function alleles. The two other mutations (c.888-1554_908+274del and c.370T>C), however, do not truncate the IMPG2 protein but only slightly alter the amino acid composition. The genomic deletion detected in the Dutch family (W01-299) results in the absence of exon 9 in the mutant *IMPG2* mRNA but does not disrupt the reading frame. At the protein level, seven amino acids (RSPKEND) are absent. These amino acids are located in the first SEA domain (named because of homology to domains present in sperm protein, enterokinase, and agrin), which contains two predicted sites for the N-linked glycosylation of IMPG2; one of these sites is located within the deleted peptide sequence (Figure 2D). In addition, the 7 amino acid peptide sequence precedes a serine-glycine motif, of which the serine residue might be the core residue to which glycosaminoglycan side chains are attached.[28] The SEA domains are frequently found in heavily glycosylated environments, and their proposed function is to regulate or assist binding to neighboring carbohydrate moieties. The first predicted SEA domain of IMPG2 resides within a predicted mucin-like sequence that is thought to play a role in the proper glycosylation of the protein. Subcellular localization assays showed that the ΔRSPKEND mutant protein is trapped in the ER, whereas the wild-type protein is targeted to the plasma membrane, suggesting that the absence of the seven amino acids impairs proper targeting of the IMPG2 protein to the cell membrane and as such might affect normal IMPG2 function in the IPM.

The missense mutation that was detected in the patient with maculopathy substitutes a leucine residue for a phenylalanine residue (p.Phe124Leu). This phenylalanine residue is highly conserved, not only in orthologous IMPG2 proteins but even in the sequence of the homologous IMPG1 proteins (Figure 2E). Phenylalanine residues have a large and bulky side chain that contains an aromatic ring, whereas leucine residues are somewhat smaller. The phenylalanine at position 124 is not located in one of the domains that are predicted to be glycosylated or to be involved in hyaluronan binding. However, given the high conservation of this residue in IMPG1 and IMPG2 proteins, in addition to the absence of this allele in ethnically matched control individuals, our data indicate that this amino acid substitution might be causative for maculopathy in the patient from family MOL0732. As such, this clinical case suggests that missense mutations in *IMPG2* might cause a less severe phenotype than nonsense mutations. The association between *IMPG2* missense mutations and maculopathy, as well as the mechanism underlying this possible genotype-phenotype correlation, requires further examination.

In a previous report, the *IMPG2* gene has been analyzed for mutations in 224 patients with various retinal diseases (mainly age-related macular degeneration, RP, and LCA), but no mutations were identified.[26] Analysis of the homologous *IMPG1* gene did not reveal mutations in patients with autosomal-dominant Stargardt-like macular dystrophy, progressive bifocal chorioretinal atrophy, and North Carolina macular dystrophy.[29] A study involving a Dutch family with autosomal-dominant benign concentric annular macular dystrophy that linked to the *IMPG1* locus identified a missense variant (p.Leu579Pro) that affects a residue that is highly conserved among IMPG1 and IMPG2 orthologs of various species and is suggested to be the causal mutation.[30]

Although the exact role of IMPG2 within the IPM is unknown, absence or impaired function of this protein probably affects the structure or function of the IPM and consequently might affect the visual processes in the

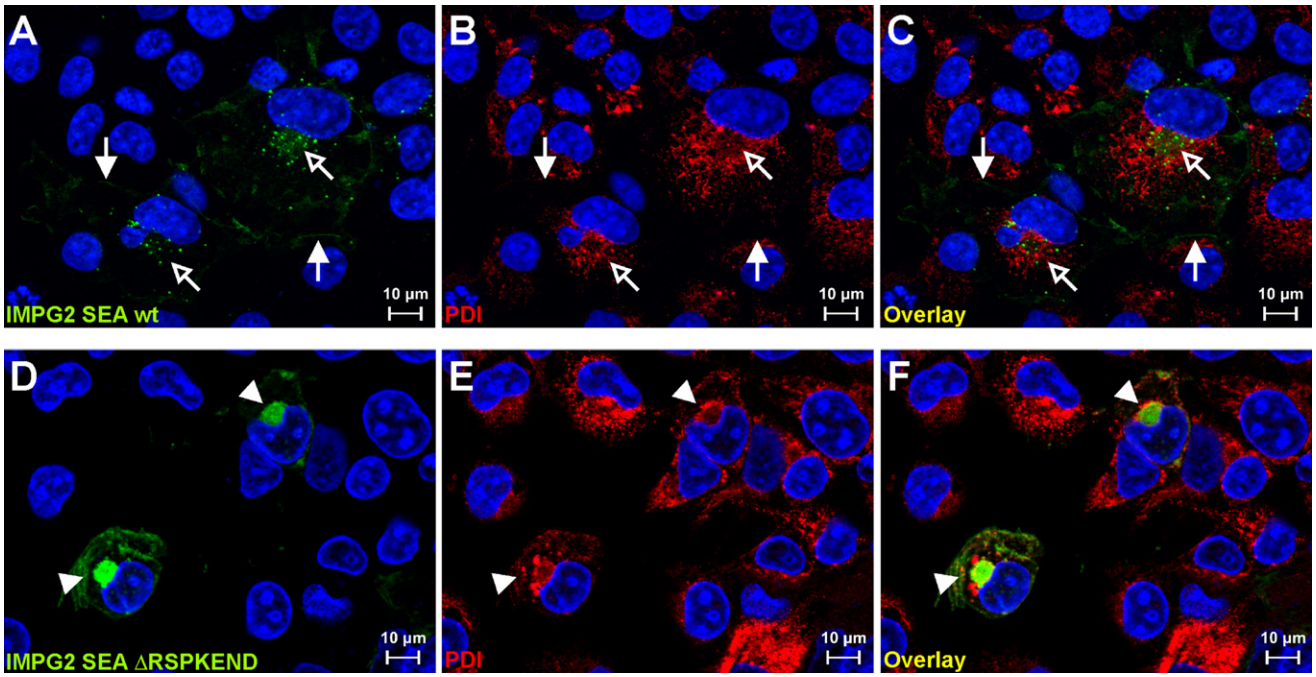


**Figure 4. Subcellular Localization of Wild-Type and ΔRSPKEND Mutant SEA-Domain Fusion Proteins**
(A–C) Images of COS-1 cells transiently transfected with a wild-type IMPG2-SEA domain fused to a signal peptide and eCFP. The wild-type fusion protein ([A], in green) localizes to vesicle-like structures in the ER ([B], PDI staining, red) and cytoplasm (open arrows) and is present at the cellular membrane (filled arrows). Nuclei are stained with DAPI (blue). (C) Overlay of (A) and (B).
(D–F) Images of COS-1 cells transiently transfected with ΔRSPKEND mutant IMPG2-SEA domain fused to a signal peptide and eCFP. The mutant fusion protein ([D], in green) accumulates in an ER-like region adjacent to the cell nucleus (arrow heads) and does not reach the plasma membrane. (E) PDI staining of the ER, red. Nuclei are stained with DAPI, blue. (F) Overlay of (D) and (E).

photoreceptor cells. The identification of *IMPG2* mutations in arRP in this report underscores the importance of the retinal ECM for maintaining retinal structure and function.

## Supplemental Data

Supplemental Data include two figures and one table and can be found with this article online at http://www.cell.com/AJHG/.

## Acknowledgments

We thank the patients and their families for participating in this study. We thank Alex Obolensky, Tamar Ben-Yosef, Saskia van der Velde-Visser, Christel Beumer, Maleeha Azam, Rolph Pfundt, Carmela Ziviello, Maria Teresa Pizzo, and the European Retinal Disease Consortium (Elfride de Baere, Carmen Ayuso, Christian Hamel, Susanne Kohl, and Rob Koenekoop) for excellent technical assistance and additional mutation analysis. This work was supported by the Foundation Fighting Blindness USA (FFB grant number BR-GE-0607-0395-HUJ to D.S. and BR-GE-0507-0381-RAD to A.I.d.H.), the Italian Ministry of Health (Progretto ricerca finalizzatta 2007), the Italian Telethon foundation, and the Yedidut 1 Research Fund.

Received: March 25, 2010
Revised: June 25, 2010
Accepted: July 11, 2010
Published online: July 29, 2010

## Web Resources

The URLs for data presented herein are as follows:

Net N-glyc server, http://www.cbs.dtu.dk/services/NetNGlyc/
Net O-glyc server. http://www.cbs.dtu.dk/services/NetOGlyc/
Online Mendelian Inheritance in Man (OMIM), http://www.ncbi.nlm.nih.gov/Omim
Retinal Information Network (Retnet), http://www.sph.uth.tmc.edu/Retnet/
SMART domain prediction software, http://smart.embl-heidelberg.de/
UCSC Genome Browser, http://www.genome.ucsc.edu

## References

1. Bundey, S., and Crews, S.J. (1984). A study of retinitis pigmentosa in the City of Birmingham. II Clinical and genetic heterogeneity. J. Med. Genet. *21*, 421–428.
2. Bunker, C.H., Berson, E.L., Bromley, W.C., Hayes, R.P., and Roderick, T.H. (1984). Prevalence of retinitis pigmentosa in Maine. Am. J. Ophthalmol. *97*, 357–365.
3. Rosenberg, T. (2003). Epidemiology of hereditary ocular disorders. Dev. Ophthalmol. *37*, 16–33.
4. Berson, E.L. (1993). Retinitis pigmentosa. The Friedenwald Lecture. Invest. Ophthalmol. Vis. Sci. *34*, 1659–1676.
5. Hartong, D.T., Berson, E.L., and Dryja, T.P. (2006). Retinitis pigmentosa. Lancet *368*, 1795–1809.
6. Dryja, T.P. (1997). Gene-based approach to human gene-phenotype correlations. Proc. Natl. Acad. Sci. USA *94*, 12117–12121.

7. Adler, A.J., and Klucznik, K.M. (1982). Proteins and glycoproteins of the bovine interphotoreceptor matrix: composition and fractionation. Exp. Eye Res. *34*, 423–434.
8. Hageman, G.S., and Johnson, L.V. (1991). Structure, composition and function of the retinal interphotoreceptor matrix. In Retinal Research, N. Osborne and G. Chader, eds. (New York: Pergamon Press), pp. 207–249.
9. Berman, E.R. (1969). Mucopolysaccharides (glycosaminoglycans) of the retina: Identification, distribution and possible biological role. Bibl. Ophthalmol. *79*, 5–31.
10. Hewitt, A.T., and Adler, R. (1989). The retinal pigment epithelium and interphotoreceptor matrix: structure and specialized function. In Retina, S.J. Ryan, ed. (St. Louis: CV Mosby Co), pp. 57–64.
11. Inatani, M., and Tanihara, H. (2002). Proteoglycans in retina. Prog. Retin. Eye Res. *21*, 429–447.
12. Enoch, J.M., and Laties, A.M. (1971). An analysis of retinal receptor orientation. II. Predictions for psychophysical tests. Invest. Ophthalmol. *10*, 959–970.
13. Lazarus, H.S., and Hageman, G.S. (1992). Xyloside-induced disruption of interphotoreceptor matrix proteoglycans results in retinal detachment. Invest. Ophthalmol. Vis. Sci. *33*, 364–376.
14. Weber, B.H., Vogt, G., Pruett, R.C., Stöhr, H., and Felbor, U. (1994). Mutations in the tissue inhibitor of metalloproteinases-3 (TIMP3) in patients with Sorsby's fundus dystrophy. Nat. Genet. *8*, 352–356.
15. Stone, E.M., Lotery, A.J., Munier, F.L., Héon, E., Piguet, B., Guymer, R.H., Vandenburgh, K., Cousin, P., Nishimura, D., Swiderski, R.E., et al. (1999). A single EFEMP1 mutation associated with both Malattia Leventinese and Doyne honeycomb retinal dystrophy. Nat. Genet. *22*, 199–202.
16. den Hollander, A.I., McGee, T.L., Ziviello, C., Banfi, S., Dryja, T.P., Gonzalez-Fernandez, F., Ghosh, D., and Berson, E.L. (2009). A homozygous missense mutation in the IRBP gene (RBP3) associated with autosomal recessive retinitis pigmentosa. Invest. Ophthalmol. Vis. Sci. *50*, 1864–1872.
17. Abd El-Aziz, M.M., Barragan, I., O'Driscoll, C.A., Goodstadt, L., Prigmore, E., Borrego, S., Mena, M., Pieras, J.I., El-Ashry, M.F., Safieh, L.A., et al. (2008). EYS, encoding an ortholog of Drosophila spacemaker, is mutated in autosomal recessive retinitis pigmentosa. Nat. Genet. *40*, 1285–1287.
18. Collin, R.W.J., Littink, K.W., Klevering, B.J., van den Born, L.I., Koenekoop, R.K., Zonneveld, M.N., Blokland, E.A., Strom, T.M., Hoyng, C.B., den Hollander, A.I., and Cremers, F.P. (2008). Identification of a 2 Mb human ortholog of Drosophila eyes shut/spacemaker that is mutated in patients with retinitis pigmentosa. Am. J. Hum. Genet. *83*, 594–603.
19. Parry, D.A., Toomes, C., Bida, L., Danciger, M., Towns, K.V., McKibbin, M., Jacobson, S.G., Logan, C.V., Ali, M., Bond, J., et al. (2009). Loss of the metalloprotease ADAM9 leads to cone-rod dystrophy in humans and retinal degeneration in mice. Am. J. Hum. Genet. *84*, 683–691.
20. Marmor, M.F., Fulton, A.B., Holder, G.E., Miyake, Y., Brigell, M., and Bach, M.; International Society for Clinical Electrophysiology of Vision. (2009). ISCEV Standard for full-field clinical electroretinography (2008 update). Doc. Ophthalmol. *118*, 69–77.
21. Rozen, S., and Skaletsky, H.J. (2000). Primer3 on the WWW for general users and for biologist programmers. In Bioinformatics Methods and Protocols: Methods in Moelcular Biology, S. Krawetz and S. Misener, eds. (Totowa, NJ: Humana Press), pp. 365–386.
22. Acharya, S., Foletta, V.C., Lee, J.W., Rayborn, M.E., Rodriguez, I.R., Young, W.S. 3rd, and Hollyfield, J.G. (2000). SPACRCAN, a novel human interphotoreceptor matrix hyaluronan-binding proteoglycan synthesized by photoreceptors and pinealocytes. J. Biol. Chem. *275*, 6945–6955.
23. Chen, Q., Lee, J.W., Nishiyama, K., Shadrach, K.G., Rayborn, M.E., and Hollyfield, J.G. (2003). SPACRCAN in the interphotoreceptor matrix of the mouse retina: molecular, developmental and promoter analysis. Exp. Eye Res. *76*, 1–14.
24. Kuehn, M.H., and Hageman, G.S. (1999). Molecular characterization and genomic mapping of human IPM 200, a second member of a novel family of proteoglycans. Mol. Cell Biol. Res. Commun. *2*, 103–110.
25. Chen, Q., Cai, S., Shadrach, K.G., Prestwich, G.D., and Hollyfield, J.G. (2004). Spacrcan binding to hyaluronan and other glycosaminoglycans. Molecular and biochemical studies. J. Biol. Chem. *279*, 23142–23150.
26. Kuehn, M.H., Stone, E.M., and Hageman, G.S. (2001). Organization of the human IMPG2 gene and its evaluation as a candidate gene in age-related macular degeneration and other retinal degenerative disorders. Invest. Ophthalmol. Vis. Sci. *42*, 3123–3129.
27. Acharya, S., Rodriguez, I.R., Moreira, E.F., Midura, R.J., Misono, K., Todres, E., and Hollyfield, J.G. (1998). SPACR, a novel interphotoreceptor matrix glycoprotein in human retina that interacts with hyaluronan. J. Biol. Chem. *273*, 31599–31606.
28. Bourdon, M.A., Krusius, T., Campbell, S., Schwartz, N.B., and Ruoslahti, E. (1987). Identification and synthesis of a recognition signal for the attachment of glycosaminoglycans to proteins. Proc. Natl. Acad. Sci. USA *84*, 3194–3198.
29. Gehrig, A., Felbor, U., Kelsell, R.E., Hunt, D.M., Maumenee, I.H., and Weber, B.H. (1998). Assessment of the interphotoreceptor matrix proteoglycan-1 (IMPG1) gene localised to 6q13-q15 in autosomal dominant Stargardt-like disease (ADSTGD), progressive bifocal chorioretinal atrophy (PBCRA), and North Carolina macular dystrophy (MCDR1). J. Med. Genet. *35*, 641–645.
30. van Lith-Verhoeven, J.J., Hoyng, C.B., van den Helm, B., Deutman, A.F., Brink, H.M., Kemperman, M.H., de Jong, W.H., Kremer, H., and Cremers, F.P.M. (2004). The benign concentric annular macular dystrophy locus maps to 6p12.3-q16. Invest. Ophthalmol. Vis. Sci. *45*, 30–35.